Journal Pre-proofs

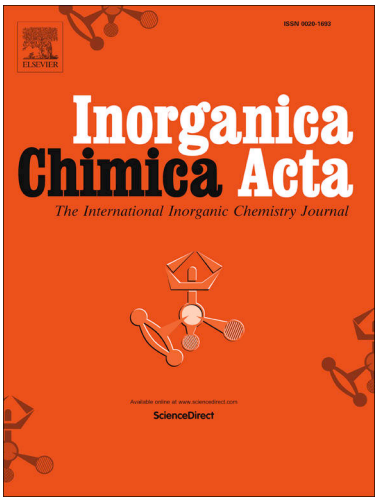

Research paper

Synthesis, characterization and biological applications of bismuth(III) complexes with aroylthiourea ligands

Marcielli Indiara de Oliveira, Gabriela Pereira Chuy, Bruno Stefanello Vizzotto, Robert Alan Burrow, Ernesto Schulz Lang, Sailer Santos dos Santos

PII: S0020-1693(20)31070-7
DOI: https://doi.org/10.1016/j.ica.2020.119871
Reference: ICA 119871

To appear in: *Inorganica Chimica Acta*

Received Date: 19 February 2020
Revised Date: 1 July 2020
Accepted Date: 4 July 2020

Please cite this article as: M.I. de Oliveira, G.P. Chuy, B.S. Vizzotto, R.A. Burrow, E.S. Lang, S.S. dos Santos, Synthesis, characterization and biological applications of bismuth(III) complexes with aroylthiourea ligands, *Inorganica Chimica Acta* (2020), doi: https://doi.org/10.1016/j.ica.2020.119871

Synthesis, characterization and biological applications of bismuth(III) complexes with aroylthiourea ligands

Marcielli Indiara de Oliveira[a], Gabriela Pereira Chuy[b], Bruno Stefanello Vizzotto[b], Robert Alan Burrow[a], Ernesto Schulz Lang[a] and Sailer Santos dos Santos[a]*

[a] *Laboratório de Materiais Inorgânicos - Departamento de Química, CCNE, UFSM, Santa Maria – RS – Brazil – 97105-900.*

[b] *Laboratório de Biologia Molecular, Universidade Franciscana - UFN, 1614 Andradas Street, Santa Maria – RS – Brazil – 97010-032.*

* Corresponding author:

E-mail: sailer.santos@ufsm.br or sailer.santos@gmail.com

Fax number: +55 55 3220 8031

Marcielli Indiara de Oliveira	0000-0003-0696-4452
Gabriela Pereira Chuy	0000-0001-6760-4851
Bruno Stefanello Vizzotto	0000-0001-6819-4081
Robert Alan Burrow	0000-0003-4909-5007
Ernesto Schulz Lang	0000-0002-6852-8667
Sailer Santos dos Santos	0000-0002-7086-8871

Abstract

This work describes the synthesis, structural characterization and biological applications of three new bismuth(III) complexes with aroylthiourea-based ligands: $[Bi(L^a)_3(HL^a)]$ (**1**), $[Bi_2(L^b)_4(\mu\text{-}L^b)_2]\cdot 2(C_3H_6O)$ (**2**), and $[Bi_6(\mu\text{-}L^c)_6(\mu_3\text{-}NO_3)_2(\mu_6\text{-}NO_3)](NO_3)_3\cdot 4H_2O$ (**3**), where HL^a = *N*-benzoyl(*N',N'*-diethylthiourea), HL^b = *N*-benzoyl(morpholinylthiourea), and H_2L^c = N^2,N^6-bis(diethylcarbamothioyl)pyridine-2,6-dicarboxamide. The ligands HL^a and HL^b were considered as monopodal, while H_2L^c as bipodal. All compounds were characterized by melting point determination, Fourier-transform infrared spectroscopy (FTIR), hydrogen and carbon-13 nuclear magnetic resonance spectroscopy (NMR), mass spectrometry (MS), elemental analysis (EA) and single-crystal X-ray diffraction (SC-XRD). Structural analysis showed that compound **1** was a mononuclear heptacoordinate complex, while compound **2** presented a dinuclear structure and compound **3** was built up by a hexanuclear framework. The proligands, the new complexes, and $Bi(NO_3)_3\cdot 5H_2O$ had their antibacterial activities evaluated against *E. coli* (ATCC 25922), *S. aureus* (ATCC 25923), and *P. aeruginosa* (ATCC 27853). The *in vitro* disk-diffusion (DD) method showed the ability of compound **2** to inhibit two types of bacteria (*P. aeruginosa* and *S. aureus*). In the results of minimum inhibitory concentration (MIC), all complexes showed significant activity against the tested microorganisms except for compound **1**. The inorganic salt used for comparison showed antibacterial activity only against *P. aeruginosa* and the ligands showed no apparent activity. Therefore, compound **2** presented the best antibacterial activity among the tested substances, and its performance was remarkable even when compared to other similar compounds found in the literature, attesting the importance of targeting bismuth(III) aroylthioureas for further research on new drugs development.

Keywords: *aroylthioureas; bismuth(III) complexes; crystal structure; antibacterial activity.*

1. Introduction

Thiourea-based molecules and their metal complexes have several pharmacological applications, especially on antimicrobial activity against pathogenic bacteria and fungi [1]. Amongst the most interesting thiourea-based ligands, aroylthioureas and their anions exhibit a rich and

very well documented coordination chemistry [2,3]. Aroylthiourea compounds of general formula Ar(C=O)NH(C=S)NR_2 (Ar = aryl; R = alkyl, aryl) (Figure 1a), constitute an important class of versatile bidentate ligands, which have hard (O), soft (S) and intermediary donor atoms (N). This structural characteristic allows these ligands to present different coordination modes, producing complexes with several distinct metals. In addition to the monopodal structure (HL') represented in Figure 1(a), aroylthiourea ligands can also be bipodal, (H_2L"), where they differ by the presence of two branches in relation to the central aromatic ring used as a spacer, as shown schematically in Figure 1(b) [4]. The removal of the acidic amidic hydrogens enhances the coordination capacity of these ligands, affording since mononuclear [5,6] to metallamacrocyclic [7-10] and heterobimetallic complexes [11-13].

INSERT **Figure 1** ABOUT HERE

Bismuth compounds are commonly used in medicine, and some have clinical applications such as treatment of syphilis (sodium/potassium bismuth tartrate, bismuth chloride, etc.), wound infections (bismuth oxide), diarrhea (bismuth subsalicylate, nitrate bismuth, etc.), and ulcer (bismuth citrate, bismuth subnitrate, etc.) [14]. In the antimicrobial activity, its main use is in the treatment of gastric disorders related to the bacterium *Helicobacter pylori* (*H. pylori*) [15], a gram-negative bacterium found in the stomach where it causes damage to epithelial cells causing gastritis and ulcers [16]. Although bismuth is considered a heavy metal, its drugs are safe if used according to the recommended dosages. Side effects from overdosing are reversible when intake is interrupted [17,18].

Recently, the broad-spectrum antimicrobial applications of bismuth-based compounds have been reviewed, including carboxylates, thiolates, phosphinic acid derivatives, and dithiocarbamate complexes [19-23]. Surprisingly, there have been no reports in the literature about bismuth complexes with aroylthiourea based proligands. Due to the extensive chemistry of aroylthiourea compounds with different types of metals with a wide variety of biological applications, and also to the well-spread uses of bismuth in commercially available drugs, we decided to investigate potential applications of bismuth(III) benzoylthioureas as antimicrobial agents. In this work, we describe the synthesis, structural characterization, and biological applications of three new bismuth(III) compounds with aroylthioureas as ligands: [Bi(L^a)$_3$(HL^a)] **1**, [Bi_2(L^b)$_4$(μ-

$L^b)_2]\cdot 2(C_3H_6O)$ **2**, and $[Bi_6(\mu\text{-}L^c)_6(\mu_3\text{-}NO_3)_2(\mu_6\text{-}NO_3)](NO_3)_3\cdot 4H_2O$ **3**, where HL^a = *N*-benzoyl(*N',N'*-diethylthiourea), HL^b = *N*-benzoyl(morpholinylthiourea), and H_2L^c = N^2,N^6-bis(diethylcarbamothioyl)pyridine-2,6-dicarboxamide (Figure 2).

INSERT **Figure 2** ABOUT HERE

2. Experimental

2.1 Materials and general instrumentation

Commercially available solvents and reagents (Sigma-Aldrich) were purified by standard methods prior to use [24]. The bismuth source, $Bi(NO_3)_3\cdot 5H_2O$, was used as received. *N*,*N*-diethylthiourea was obtained from acidic hydrolysis of *in situ* prepared *N*-benzoyl(*N',N'*-diethylthiourea) [25]. Synthetic manipulations involving air-sensitive compounds were carried out using a standard argon atmosphere. CHNS elemental analyses were performed at a Heraeus Vario EL microanalysis instrument. Melting points (m.p.) were recorded using a MicroQuímica, MQAPEF-301 digital melting point apparatus and were not corrected. Fourier-transform infrared (FTIR) spectra, in attenuated total reflectance (ATR) sampling mode, were recorded on a Bruker Vertex 70 spectrometer with a Bruker Platinum ATR accessory, equipped with a diamond crystal window. A total of 32 scans were performed at 4 cm^{-1} resolution in the 4000-400 cm^{-1} spectral range and then converted to transmission mode. ^1H and ^{13}C nuclear magnetic resonance (NMR) spectra were recorded on a Bruker DPX-400 or on a Bruker Avance III HD-600 spectrometers. $CDCl_3$, DMSO-d_6, and acetone-d_6 were used as solvents and TMS as the internal reference. Chemical shifts are reported in parts per million (δ, ppm) and were referenced to the residual solvent peak. Multiplicities are expressed as: s (singlet), t (triplet), q (quartet), m (multiplet), and br (broad). The electrospray-ionization Fourier-transform ion-cyclotron-resonance (ESI-FTICR) mass spectrometric (MS) experiments were performed with a Varian IonSpec QFT-7 FTICR mass spectrometer in positive mode. All MS results are given in the form: *m/z*, assignment (M stands for the corresponding molecular ion peak).

2.2 Single-crystal X-ray diffractometry (SC-XRD)

Data were collected on a Bruker D8 Venture diffractometer equipped with an Incoatec IμS high brilliance Mo-Kα X-ray tube with two-dimensional Montel micro-focusing optics and a Photon 100 detector. The structures were solved by dual space methods with Bruker SHELXTL XT [26]. Fourier-difference map analyses yielded the positions of the non-hydrogen atoms, and

refinements were carried out with the Bruker SHELXTL XL package [27]. All refinements were made by full-matrix least-squares on F^2 with anisotropic displacement parameters for all non–hydrogen atoms. Hydrogen atoms were included in the refinement in calculated positions according to the molecular skeletons. Drawings were done using Crystal Impact Diamond 3 [28]. Crystal data and more details of the data collection and refinements of the bismuth(III) complexes **1, 2,** and **3** are presented in Table S1 of Supplementary Information file.

2.3 Disk Diffusion Assay (DD)

The antimicrobial susceptibility was performed by the agar disk diffusion method in cation adjusted Mueller-Hinton agar (CAMH) as recommended by the Clinical and Laboratory Standards Institute (CLSI) [29], with the microorganisms *Escherichia coli* (ATCC 25922), *Staphylococcus aureus* (ATCC 25923) and *Pseudomonas aeruginosa* (ATCC 27853). Isolated pure colonies were transferred into a sterile saline solution to form homogenous bacterial suspensions, in a standard turbidity inoculum equivalent to 0.5 McFarland (1×10^8 CFU mL^{-1}), then poured over the agar plates and allowed to dry for 5 min. Sterile filter paper disks (Whatman No. 1, diameter = 6 mm) were placed over the agar surface and impregnated with 10 μL of a solution of each compound (freshly dissolved in deionized water at 0.01 *M*), and incubated for 24 h at 37 °C. Cefotaxime (30 μg) and Ceftazidime (30 μg) disks were used as positive controls. The inhibition zones were measured in millimeters as the diameter of the growth-free zones. All tests were performed in triplicate.

2.4 Minimal Inhibitory Concentration (MIC)

The broth microdilution method was used to determine the MIC according to CLSI [29], as described previously. All analyses were performed in triplicate. Twofold serial dilutions of compounds were prepared directly in a microtiter plate containing Mueller Hinton broth to obtain concentrations ranging from 10 m*M* to 0.019 m*M*. Bacterial inoculum was added at a final concentration of 5×10^4 CFU mL^{-1} per well. Plates were then covered and incubated for 24 h at 37 °C. The MIC of the samples was detected using spectrophotometric reading at 595 nm after the addition of 20 μL triphenyl-tetrazolium chloride (TTC) solution (0.02 g mL^{-1}) incubated at 37 ºC for 2 h. The growth of bacteria changes the dye from colorless to red, indicating positive

growth, whereas the colorless indicates growth inhibition. MIC was defined as the lowest sample concentration which prevented this change and exhibited inhibition of microorganism growth.

2.5 Synthetic procedures

2.5.1 Synthesis of the ligands

The syntheses of the monopodal ligands *N*-benzoyl(*N',N'*-diethylthiourea) (HL^a) and *N*-benzoyl(morpholinylthiourea) (HL^b) were adapted from Douglass and Dains [30]. The preparation of the bipodal ligand N^2,N^6-bis(diethylcarbamothioyl)pyridine-2,6-dicarboxamide (H_2L^c) was adapted from reported procedures [31-33].

2.5.1.1 Synthesis of HL^a and HL^b

In a 250 mL three-neck round-bottom flask, equipped with a magnetic stirring system and reflux condenser, ammonium thiocyanate (7.61 g, 100 mmol) was suspended in 100 mL of dry acetone. Then, 12.0 mL of benzoyl chloride (14.8 g, 105 mmol) was slowly added dropwise. During the addition, the mixture changed from colorless to yellow. After completion of the addition, the system was heated to reflux for 2 h. The reaction mixture was cooled with an ice bath, and 120 mmol of the corresponding amine (see below) was added dropwise. After the end of the addition, the system was kept at room temperature with magnetic stirring for 2 h. Afterwards, 200 mL of a 6 mol L^{-1} HCl solution was added to the reaction mixture and extraction was performed with ethyl acetate (3 × 100 mL). The solvent was removed by a rotatory evaporator, and the product was purified by recrystallization from a mixture of ethyl ether and methanol (4:1). The crystalline product was dried under high vacuum for 4 h.

HL^a: 12.0 mL of diethylamine (8.78 g). **Yield:** 61.5% (14.5 g; 61.5 mmol); $C_{12}H_{16}N_2OS$ (F.W.= 236.33 g mol^{-1}); **Elem. Anal.:** *Calcd*: C = 60.99%; H = 6.82%; N = 11.85%; S = 13.57%; *Found*: C = 60.37%; H = 6.72%; N = 12.11%; S = 13.24%; **m.p.:** 102 °C; **FTIR** (ATR, cm^{-1}): ν(N-H) 3264; ν(C=O) 1651; **^{1}H NMR** (DMSO-D_6; δ/ppm; *J*/Hz): 10.33 (br, 1H, NH); 7.93 (d, 2H, C*H*, *J* = 7.14); 7.59 (t, 1H, C*H*, *J* = 7.35); 7.50 (t, 2H, C*H*, *J* = 7.72); 3.95 (q, 2H, CH_2, *J* = 6.94); 3.52 (q, 2H, CH_2, *J* = 7.04); 1.25 (t, 3H, CH_3, *J* = 7.00); 1.18 (t, 3H, CH_3,

J = 7.10); **^{13}C NMR** (DMSO-D_6; δ/ppm): 180.98 (*C*=S), 164.52 (*C*=O), 133.45 (*C*H); 132.73 (*C*H); 128.92 (*C*H); 128.55 (*C*H); 48.99 (*C*H_2); 47.71 (*C*H_2); 13.81 (*C*H_3); 11.58 (*C*H_3).

HL^b: 11.0 mL of morpholine (10.8 g). **Yield:** 67.5% (16.9 g; 67.5 mmol); $C_{12}H_{14}N_2O_2S$ (F.W.= 250.32 g mol^{-1}); **Elem. Anal.:** *Calcd*: C = 57.58%; H = 5.64%; N = 11.19%; S = 12.81%; *Found*: C = 57.43%; H = 5.63%; N = 10.99%; S = 12.73%; **m.p.:** 149 ºC; **FTIR** (ATR, cm^{-1}): ν(N-H) 3236; ν(C=O) 1662; **^{1}H NMR** (acetone-D_6; δ/ppm; *J*/Hz): 9.68 (br, 1H, NH); 8.00 (d, 2H, C*H*, *J* = 7.21); 7.62 (t, 1H, C*H*, *J* = 7.43); 7.52 (t, 2H, C*H*, *J* = 7.80); 4.21 (br, 2H, CH_2); 3.76 (br, 4H, CH_2); 3.69 (br, 2H, CH_2); **^{13}C NMR** (DMSO-D_6; δ/ppm): 180.85 (*C*=S); 164.55 (*C*=O); 133.91 (*C*H); 133.42 (*C*H); 129.39 (*C*H); 129.07 (*C*H); 66.75 (*C*H_2); 52.55 (*C*H_2); 51.91 (*C*H_2).

2.5.1.2 Synthesis of **H_2L^c**

In a 250 mL three-neck round-bottom flask, equipped with a magnetic stirring system and reflux condenser, 9.30 mL of triethylamine (6.75 g; 66.7 mmol) were added dropwise into a solution of *N,N*-diethylthiourea (5.00 g; 37.8 mmol) in 100 mL of dry acetone. A suspension of pyridine-2,6-dicarbonyl dichloride (3.86 g; 18.9 mmol) in 50.0 mL of anhydrous acetone was slowly added dropwise. After completion of the addition, the system was stirred for 1 h at room temperature (r.t.). Then, the system was kept between 50 – 60 ºC with an oil bath for 2 h. After cooling down to r.t., the reaction mixture was filtered, and the filtrate was concentrated to dryness. The brown oily product was washed several times with an ethyl ether/methanol 10:1 solution, and the resulting white solid was collected by filtration and dried under high vacuum for 4 h.

H_2L^c: Yield: 68.0% (5.09 g; 12.9 mmol); $C_{17}H_{25}N_5O_2S_2$ (F.W.= 395.54 g·mol^{-1}); **Elem. Anal.:** *Calcd*: C = 51.62%; H = 6.37%; N = 17.71%; S = 16.21%; *Found*: C = 51.64%; H = 6.36%; N = 17.63%; S = 16.07%; **m.p.:** 179 ºC; **FTIR** (ATR, cm^{-1}): ν(N-H) 3265; ν(C=O) 1672; **^{1}H NMR** (DMSO-D_6; δ/ppm; *J*/Hz): 11.29 (s, 2H, N*H*); 8.33 (m, 2H, *m*-Py); 8.28 (m, 1H, *p*-Py, *J* = 8.65); 4.00 (q, 4H, CH_2, *J* = 7.03); 3.59 (q, 4H, CH_2, *J* = 7.11); 1.29 (t, 6H, CH_3, *J* = 7.05); 1.20 (t, 6H, CH_3, *J* = 7.14); **^{13}C NMR** (DMSO-D_6; δ/ppm): 180.28 (*C*=S); 160.61 (*C*=O); 148.34 (*C*H); 140.62 (*C*H); 126.44 (*C*H); 47.89 (*C*H_2); 47.25 (*C*H_2); 14.09 (*C*H_3); 11.56 (*C*H_3).

2.5.2 Synthesis of the bismuth(III) complexes

Bismuth(III) complexes with the selected ligands were obtained using a similar protocol. A general optimized procedure is described below.

The ligand was dissolved in 4.0 mL of solvent under magnetic stirring. After complete dissolution, three drops of NEt_3 were added.* A solution of $Bi(NO_3)_3 \cdot H_2O$ (0.048 g, 0.10 mmol) in 2.0 mL of solvent was added dropwise to the first solution causing the formation of a yellow solution to be observed. The reaction mixture was kept under magnetic stirring for 1 h in open atmosphere. The solution was filtered, and crystals suitable for SC-XRD measurements were obtained after slow evaporation of the mother liquor.

* Ligand H_2L^c required gentle heating for dissolution, and no NEt_3 was added.

[Bi(L^a)$_3$(HL^a)] (1) - Ligand: HL^a (0.070 g, 0.30 mmol); **Solvent:** EtOH; **Yield:** 86% (0.073 g; 64 mmol); $C_{48}H_{62}BiN_8O_4S_4$ (F.W.= 1151.29 g·mol^{-1}); **Elem. Anal.** *Calcd*: C = 50.08%; H = 5.34%; N = 9.73%; S = 11.14%; *Found*: C = 50.25%; H = 5.34%; N = 9.77%; S = 11.16%; **m.p.:** 110 ºC; **FTIR** (ATR, cm^{-1}): ν(C=O) = 1682; ν(C=O) = 1494; ν(C=S) = 1222; **ESI$^+$-MS:** 1151.2613 $[M+H]^+$ (*Calcd*: 1151.3575); 1150.2808 $[M]^+$ (*Calcd*: 1150.3502); 679.1599 $[Bi(L^a)_2]^+$ (*Calcd*: 679.1609); **^{1}H NMR** ($CDCl_3$; δ/ppm; *J*/Hz): 8.66 (br, 1H, N*H*); 7.83 (d, 8H,C*H*, *J* = 7.54); 7.54 (t, 4H, C*H*, *J* = 7.41); 7.43 (t, 8H, C*H*, *J* = 7.65); 3.13 (q, 16H, CH_2, *J* = 7.33); 1.29 (t, 24H, CH_3, *J* = 7.34); **^{13}C NMR** ($CDCl_3$; δ/ppm): 179.49 (*C*=S), 163.49 (*C*=O), 133.08 (*C*H); 132.47 (*C*H); 128.92 (*C*H); 127.93 (*C*H); 65.85 (*C*H_2); 52.11 (*C*H_2); 46.59 (*CH*$_2$); 8.69 (*C*H_3).

[Bi$_2$(μ-L^b)$_2$(L^b)$_4$]·2(CO)Me$_2$ (2) - Ligand: HL^b (0.075 g, 0.30 mmol); **Solvent:** (CO)Me_2; **Yield:** 90% (0.091 g; 0.05 mmol); $C_{78}H_{90}Bi_2N_{12}O_{14}S_6$ (F.W.= 2029.93 g·mol^{-1}); **Elem. Anal.**: *Calcd*: C = 46.15%; H = 4.47%; N = 8.28%; S = 9.48%; *Found*: C = 45.41%; H = 4.28%; N= 8.73%; S = 9.51%; **m.p.:** 160 ºC; **FTIR** (ATR, cm^{-1}): $\nu(C=O)_{acetone}$ = 1702; ν(C=O) = 1484; ν(C=S) = 1222; **ESI$^+$-MS:** 1663.2958 $[M-(L^b)]^+$ (*Calcd*: 1663.3096); 707.1156 $[Bi(L^b)_2]^+$ (*Calcd*: 707.1199); **^{1}H NMR** (acetone-D_6; δ/ppm; *J*/Hz): 8.01 (d, 6H, C*H*, *J* = 7.53); 7.63 (t, 3H, C*H*, *J* = 7.45); 7.53 (t, 6H, C*H*, *J* = 7.74); 2.83 (br, 24H, CH_2); **^{13}C NMR** (acetone-D_6; δ/ppm): 179.11 (*C*=S); 163.21 (*C*=O); 133.36 (*C*H); 130.62 (*C*H); 129.36 (*C*H); 129.04 (*C*H); 66.94 (*C*H_2); 66.70 (*C*H_2).

$[Bi_6(\mu\text{-}L^c)_6(\mu_3\text{-}NO_3)_2(\mu_6\text{-}NO_3)](NO_3)_3{\cdot}4H_2O$ (3) - Ligand: H_2L^c (0.039 g, 0.10 mmol); **Solvent:** MeOH; **Yield:** 52% (0.035 g; 0.0086 mmol); $C_{102}H_{146}Bi_6N_{36}O_{34}S_{12}$ (F.W.= 4059.13 g/mol); **Elem. Anal.** *Calcd:* C = 30.18%; H = 3.63%; N = 12.42%; S = 9.48%; *Found:* C = 29.10%; H = 3.35%; N = 12.50%; S = 8.88%; **m.p.:** 228 ºC; **FTIR** (ATR, cm^{-1}): ν(O-H) 3430,05; ν(C=O) 1642; ν(C-O) 1520; ν(N-O) 1331, 1346; **ESI^+-MS:** 2594.3883 $[Bi_4(L^d)_4(NO_3)_3]^+$ (*Calcd*: 2594.4018); 1930.2931 $[Bi_3(L^d)_3(NO_3)_2]^+$ (*Calcd*: 1930.3042); 1266.2003 $[Bi_2(L^d)_2(NO_3)]^+$ (*Calcd*: 1266.2067); 602.1066 $[Bi(L^d)]^+$ (*Calcd*: 602.1092; **^{1}H NMR** (DMSO-D_6; δ/ppm; *J*/Hz): 7.95 (d, 12H, *m*-Py, *J* = 7.06); 7.60 (t, 6H, *p*-Py, *J* = 7.14); 3.12 (q, 24H, C*H*$_2$, *J* = 7.28); 1.20 (t, 36H, C*H*$_3$, *J* = 7.29); **^{13}C NMR** (DMSO-D_6; δ/ppm): 179.91 (*C*=S); 163.90 (*C*=O); 132.56 (*C*H); 132.21 (*C*H); 128.14 (*C*H); 65.47 (*C*H_2); 50.47 (*C*H_2); 45.93 (*C*H_2); 8.50 (*C*H_3); 8.43 (*C*H_3).

3. Results and discussions

3.1. Molecular and crystal structures

Compounds **1**-**3** were obtained as crystalline materials and had their crystal and molecular structures determined.

3.1.1. Compound **1**

Compound **1**, $[Bi(L^a)_3(HL^a)]$, crystallized in the monoclinic system, with space group *C*2/*c*, forming a heptacoordinate Bi^{III} complex. It was possible to observe that the ligand acquired two different coordination modes in the structure: anionic bidentate coordination mode, where three L^a-κ^2*S*,*O* chelating ligands were coordinated to the metal, and one monodentate coordination, where only the sulfur atom of a neutral HL^a-κ*S* was coordinated to the Bi^{III} ion (Figure 3(a)). This asymmetry in the behavior of the ligands occurred due to a change in the configuration of one of the ligands, which underwent a rotation around the *sp*^{3} nitrogen atom of the amide residue, changing the torsion angle of the system -(CO)NH(CS)-. This change in conformation caused the atoms of oxygen and sulfur to be very distant, preventing the formation of the fourth chelate. In complex **1**, the geometry around bismuth was a highly distorted pentagonal bipyra-

mid (PBPY-7), where three oxygen and two sulfur atoms were occupying the equatorial positions (O1, O2, O3, S1, S3) while the axial positions were occupied by two sulfur atoms (S2, S4) (Figure 3(b)).

INSERT **Figure 3** ABOUT HERE

The bismuth(III) ion has an ionic radius large enough to form complexes with greater numbers of coordination, as already reported in some examples in the literature, e.g. 7 [34], 8 [35] and 9 [36]. The three L^a-κ^2*S,O* chelating ligands presented Bi-O bond lengths range between 2.3704(03) - 2.4072(03) Å, and Bi-S bond lengths between 2.6192(12) - 2.8462(11) Å, while the seventh coordination consisted of a bond of a sulfur atom from an adjacent neutral ligand (3.2147(11) Å), much longer than the Bi-S bonds observed for the chelating ligands. The high degree of distortion of the pentagonal bipyramidal geometry can be related to the stereochemical activity of the Bi^{III} lone pair that led to an hemidirected coordination environment [37- 41]. This hemidirected coordination was also evidenced by the relatively high values found for the O2-Bi1-S4 and S1-Bi1-S3 angles (118.792(2) – 137.643(1)°), which made the O2-S3-S4-S1 quadrilateral system almost planar (torsion angle -12.360(1)°). Selected bond lengths and angles are shown in Table 1.

INSERT **Table 1** ABOUT HERE

3.1.2. Compound **2**

Compound **2**, **$[Bi_2(\mu\text{-}L^b)_2(L^b)_4]\cdot 2(CO)Me_2$**, crystallized in the triclinic system with space group $P\bar{1}$ as a dinuclear Bi^{III} complex that had six anionic ligands derived from *N*-benzoyl-morpholinylthiourea, and two acetone molecules as solvates in its molecular structure. Four L^b moieties behaved as κ^2*S,O* chelating ligands while the two remaining acted as μ-L^b-(1κ^2*O,S*,2κ*S*) and μ-L^b-(1κ*S*,2κ^2*O,S*) ligands, respectively (Figure 4 (a)).

The two Bi^{III} ions presented equivalent coordination spheres. The bismuth coordination number was also seven in a strongly distorted pentagonal bipyramidal geometry, where three oxygen and two sulfur atoms (O11, O21, O31, S11, and S33) were occupying the equatorial positions while the axial positions were occupied by two sulfur atoms (S22, S33') (Figure 4(b)).

INSERT **Figure 4** ABOUT HERE

As well as for **1**, the hemidirected pentagonal bipyramidal coordination in **2** was due to the effect of the stereochemically active Bi^{III} electron lone pair, and the distortion, in this case, was also enhanced due to the sterical hindrance imposed by the bridging ligands. The O21-Bi1-S33' and S11-Bi1-S33 bond angles were very large for a PBPY-7 coordination (137.750(5) and 146.157(3)°, respectively), which made the system O21-S33-S33'-S11 almost planar (torsion angle –9.520(6)°). Selected bond distances and angles are shown in Table 2, where Bi-O bond lengths range between 2.3140(14) and 2.4998(17) Å and the chelate Bi-S bond lengths between 2.6616(07) and 2.6955(07) Å, while the sixth and seventh coordination positions were constituted by μ-S bonds of bridging ligands with bond lengths between 3.0946(07) - 3.1542(07) Å.

INSERT **Table 2** ABOUT HERE

3.1.3. Compound **3**

Compound **3**, $[Bi_6(\mu\text{-}L^c)_6(\mu_3\text{-}NO_3)_2(\mu_6\text{-}NO_3)](NO_3)_3{\cdot}4H_2O$, crystallized in the monoclinic system, with space group $P2_1/n$. The molecular structure of **3** consisted in a hexanuclear cluster built up by six dianionic bridging L^c ligands connecting the Bi^{III} ions in a distorted trigonal antiprismatic structure. Three nitrate ions were encapsulated in the central void of this framework, with the other three nitrate ions acting as counterions, and four water molecules as solvates. The encapsulated nitrate ions assembled a very intricate bonding net with the Bi^{III} ions, forming μ_3 (marginal nitrates) and μ_6 (central nitrate) systems. The central nitrate ion was situated on a crystallographic inversion center and exhibited a static disorder, being 50% eclipsed to each vicinal nitrate moiety. Figure 5 shows the structure of the cationic fragment of compound **3** and the nitrate ions encapsulated in its central void.

INSERT **Figure 5** ABOUT HERE

The L^c moieties intercalated the Bi^{III} ions in pairs showing a κ^4*O,N,N',S* tetradentate coordination to one cation and a κ^2*O,S'* bidentate coordination to the second cation, in which both Bi^{III} ions were connected by the same oxygen atom. This coordination scheme was possible due to a modification in the conformation of one of the amide residues of the ligand side chains (Figure

6). This structure was quite different from those observed for indium(III) complexes with similar ligands [41, 42].

INSERT **Figure 6** ABOUT HERE

There were three crystallographic independent Bi^{III} ions: Bi1, Bi2, and Bi3. Atom Bi1 was nonacoordinate, while Bi2 and Bi3 were decacoordinate. For all Bi^{III} species, the κ^4*O,N,N',S* tetradentate chelate rings built up a hemidirected pentagonal pyramidal coordination in which the fifth basal position was completed by an oxygen atom from a κ^2*O,S'* chelate provided by a second L^c ligand, and the apical position was occupied by the sulfur atom of this same second chelate ring. The complete coordination spheres were holodirected if taking into account the secondary bonds with the encapsulated nitrate groups. The coordination environments of the independent Bi^{III} species are depicted in Figure 7.

INSERT **Figure 7** ABOUT HERE

This tangled structure imposed a high steric hindrance that introduced longer bond lengths than the observed for the other complexes, especially for the Bi-O bonds. The Bi-O bonds from the L^c skeleton were in the range of 2.6162(3) - 2.6761(3) Å, while longer Bi···O contacts provided by the enclosed nitrate groups were in the range of 2.8025(3) - 3.1825(2) Å. The coordinate bonds between the Bi-N and Bi-S atoms had bond length ranges between 2.3100(04) - 2.5403(4) Å and 2.6150(16) – 2.7635(15) Å, respectively. The basal N-Bi-S bond angles were in the range of 60.616(5) - 61.119(5)º while the apical N-Bi-S bond angles were between 69.432(5) - 92.431(5)º, which were significantly different due to the irregularity of the bond framework. Selected bond lengths and angles are shown in Table 3.

INSERT **Table 3** ABOUT HERE

3.2. Fourier-transform infrared (FTIR) spectroscopy

Fourier-transform infrared (FTIR) spectra of all compounds are similar. The strong NH stretching bands occurred between 3110-3265 cm^{-1} for the free ligands and were not observed in the complexes, except for **1** that presented a weak peak at 3243 cm^{-1} since it had one neutral HL^a molecule coordinated to bismuth(III). The strong C=O stretching bands were observed between 1651-1688 cm^{-1} for the free ligands. A strong red shift was observed for these bands in the

complexes spectra (1484-1520 cm^{-1}) as a result of coordination. A similar bathochromic effect was observed for the C=S stretching modes, that relied on 1266-1278 cm^{-1} for the free ligands and in 1245-1258 cm^{-1} for the complexes [43, 44]. For compound **3**, nitrate modes were observed in 1331 and 1346 cm^{-1} [45]. Table 4 summarizes the main bands observed in the FTIR spectra and the respective assignment attempts of the synthesized ligands and complexes for comparison.

INSERT **Table 4** ABOUT HERE

3.3. ^{1}H and ^{13}C Nuclear Magnetic Resonance (NMR) spectroscopy

Essentially, the ^{1}H NMR spectra of the proligands and their corresponding complexes were quite similar. Also, no significant differences were observed in the ^{13}C NMR spectra of the proligands in comparison to their respective complexes.

Comparing the ^{1}H NMR spectra of HL^{a} and **1**, the chemical shifts observed for the complex were slightly shielded in comparison to the ligand, especially for the N-H acidic hydrogen. However, a direct discussion regarding the coordination effect was not possible because these spectra were collected using different solvents. The CH_3-triplets (1.18 and 1.25 ppm) and the CH_2-quartets (3.52 and 3.95 ppm) of the ethyl groups appeared split for HL^{a}, but only one triplet (1.29 ppm) and one quartet (3.13 ppm) were observed for complex **1**, which can be related to a decrease in the degree of freedom of the individual methyl and methylene moieties upon coordination.

Comparing the ^{1}H NMR spectra of HL^{b} and **2**, the main difference was related to the CH_2-morpholinyl resonances: in HL^{b}, these resonances were distributed between 3.69-4.21 ppm, while in **2** they were apparently merged in one single broad signal centered at 2.83 ppm (residual water peak could overlap the other peak). The aromatic region of the spectra was almost identical, and the NH signal observed at 9.68 ppm for HL^{b} was absent in complex **2**.

The ethyl moiety resonances in the ^{1}H NMR spectra of H_2L^{c} and **3** followed the same trend observed for HL^{a} and **1**: CH_3-triplets (1.20 and 1.29 ppm) and CH_2-quartets (3.59 and 4.00 ppm) were split for the ligand, but only one resonance of each group was observed for the complex (triplet: 1.20 ppm; quartet: 3.12 ppm). The H-aromatic resonances were not resolved for H_2L^{c} (multiplets at 8.28 and 8.33 ppm), but a clear doublet (7.95 ppm) and a triplet (7.60 ppm) were observed for the complex **3**. The NH resonance observed at 11.29 ppm for H_2L^{c} was absent in the ^{1}H NMR spectrum of **3**, as expected.

3.4. Antibacterial activity

Given the well-known antimicrobial activity of bismuth compounds, we tested the inhibition ability of the synthesized ligands, complexes as well as the starting salt $Bi(NO_3)_3 \cdot 5H_2O$ against the selected two Gram-Negative (*E. coli* and *P. aeruginosa)* and Gram-Positive (*S. aureus)* bacteria by the disc diffusion and broth microdilution assays (Table 5). Based on the disc diffusion assay, only compound **2** showed stronger inhibiting bacterial abilities producing inhibition of zones of 13.0 mm and 12.0 mm for *P. aeruginosa* and *S. aureus*, respectively. These data indicated that the antibacterial performance of **2** was about three times greater than those found in the literature for copper compounds containing similar ligands [46]. This pronounced increase in activity can be attributed to the morpholine ring present in the structure in which the heterocyclic compounds activate biological activity [46].

INSERT **Table 5** ABOUT HERE

For the antimicrobial activities evaluated by broth microdilution assay, the tested compounds presented distinct behaviors. Bismuth(III) nitrate showed activity only against *P. aeruginosa*, while the ligands did not show any apparent activity. A minimum inhibitory concentration (MIC) for bismuth compounds is between 0.019 and 5.0 μg mL^{-1}. Compound **1** does not demonstrate satisfactory activity for the tested bacteria, while compounds **2** and **3** demonstrate interesting activities. Among them, compound **2**, was the most active for the three different types of bacteria (*E. coli* = 0.156 μg mL^{-1}, *P. aeruginosa* = 1.250 μg mL^{-1}, and *S. aureus* = 0.019 μg mL^{-1}). Compound **3** was shown to be more efficient against *P. aeruginosa* and *S. aureus* with a minimum inhibition concentration of 2.5 μg mL^{-1} for both.

4. Conclusions

The new bismuth(III) aroylthioureas complexes were synthesized from monopodal (HL^a and HL^b) and bipodal (H_2L^c) ligands with the following compositions $[Bi(L^a)_3(HL^a)]$ (**1**), $[Bi_2(L^b)_4(\mu\text{-}L^b)_2]\cdot 2(C_3H_6O)$ (**2**), and $[Bi_6(\mu\text{-}L^c)_6(\mu_3\text{-}NO_3)_2(\mu_6\text{-}NO_3)](NO_3)_3\cdot 4H_2O$ (**3**). The synthesized ligands and complexes were satisfactorily characterized by different analytical methodologies. Single-crystal X-ray diffraction studies were carried out for the crystalline compounds **1**, **2**, and **3**, revealing mononuclear, dinuclear, and hexanuclear structures, respectively.

Antimicrobial activity in the DD assay showed that compound **2** presented a significant inhibition zone against two types of bacteria (*P. aeruginosa* and *S. aureus*) with a performance close to three times better than those found for similar compounds against the same bacteria. In the MIC test, all synthesized complexes proved to be efficient against the three selected bacteria (*E. coli*, *S. aureus*, and *P. aeruginosa*). Compound **2** presented the best values, even when compared to other bismuth compounds found in the literature, attesting the importance of targeting bismuth(III) aroylthioureas for further research on new drugs development.

5. Abbreviations

ATCC	American type culture collection
ATR	Attenuated total reflectance
Calcd.	Calculated
CAMH	Cation adjusted Mueller-Hinton agar
CCDC	Cambridge Crystallographic Data Centre
CFU	Colony-forming unit
CLSI	Clinical and Laboratory Standards Institute
DD	Disk Diffusion Assay
DMSO	Dimethylsulfoxide
Elem. Anal.	Elemental analysis
ESI-FTICR	Electrospray-ionization Fourier-transform ion-cyclotron-resonance
ESI-MS	Electrospray-ionization mass spectrometry
FTIR	Fourier-transform infrared spectroscopy
F.W.	Formula weight
HL^a	*N*-benzoyl(*N',N'*-diethylthiourea)
HL^b	*N*-benzoyl(morpholinylthiourea)
H_2L^c	N^2,N^6-bis(diethylcarbamothioyl)pyridine-2,6-dicarboxamide
M	molecular ion peak
M	molar (mol L^{-1})
MIC	Minimal Inhibitory Concentration
m.p.	Melting point
MS	Mass spectrometry
m/z	mass/charge ratio
NMR	Nuclear magnetic resonance spectroscopy
PBPY-7	Seven-coordination pentagonal bipyramid
ppm	parts per million
r.t.	room temperature
SC-XRD	Single-crystal X-ray diffractometry
TMS	Tetramethylsilane
TTC	Triphenyl-tetrazolium chloride

6. Supplementary data

A crystallographic data table, ellipsoid representations, and spectroscopic data are available free of charge as electronic supplementary information. CCDC 1984604, 1984603, and 1984605 contain the supplementary crystallographic data for the complexes **1**, **2**, and **3**, respectively. These data can be obtained free of charge via http://www.ccdc.cam.ac.uk/conts/retrieving.html, or from the Cambridge Crystallographic Data Centre, 12 Union Road, Cambridge CB2 1EZ, UK; fax: (+44) 1223–336–033; or e–mail: deposit@ccdc.cam.ac.uk.

7. CRediT author statement

Marcielli Indiara de Oliveira: Investigation, Validation, Formal analysis, **Gabriela Pereira Chuy:** Investigation, Validation, **Bruno Stefanello Vizzotto:** Supervision, Methodology, Resources, Writing - Review & Editing, **Robert Alan Burrow:** Formal analysis, Writing - Review & Editing, **Ernesto Schulz Lang:** Funding acquisition, Resources, Writing - Review & Editing, **Sailer Santos dos Santos:** Funding acquisition, Supervision, Resources, Methodology, Conceptualization, Project administration, Writing - Original Draft, Writing - Review & Editing.

8. Declaration of interest

The authors declare that they have no known competing financial interests or personal relationships that could have appeared to influence the work reported in this paper.

9. Acknowledgments

We would like to thank the financial agencies: Brazilian Research Councils (CNPq), Coordenação de Aperfeiçoamento de Pessoal de Nível Superior via CAPES-PrInt, and CAPES-PROEX programs- Finance Code 001, and also CAPES/PROBRAL (88881.144118/2017-01). M.I.O. gratefully acknowledges a scholarship from PPGQ/UFSM CAPES/PROEX program. S.S.S. gratefully acknowledges grants sponsored by FIPE/CCNE/UFSM projects. The X-ray diffractometer and the FTIR spectrometer were purchased with funding from FINEP/CT-Infra.

10. References

[1] R.K. Mohapatra, P.K. Das, M. K. Pradhan, M. M. El-Ajaily, D. Das, H.F. Salem, U. Mahanta, G. Badhei, P.K. Parhi, A.A. Maihub, M. Kudrat-E-Zahan, Comment. Inorg. Chem. (2019) 01-61.
https://doi.org/10.1080/02603594.2019.1594204

[2] K.R. Koch, Coord. Chem. Rev. 216–217 (2001) 473–488.
https://doi.org/10.1002/chin.200137269

[3] A. Saeed, M.N. Mustafa, M. Zain-ul-Abideen, G. Shabir, M.F. Erben, U. Flörke, J. Sulfur Chem. 40 (2019) 312-350.
https://doi.org/10.1080/17415993.2018.1551488

[4] B. O'Reilly, A.M. Plutín, H. Pérez, O. Calderón, R. Ramos, R. Martínez, R.A. Toscano, J. Duque, H. Rodríguez-Solla, R. Martínez-Alvarez, M. Suárez, N. Martín, Polyhedron 36 (2012) 133-140.
https://doi.org/10.1016/j.poly.2012.02.008

[5] M. Sternberg, J. Rust, C.W. Lehmann, F. Mohr, Helv. Chim. Acta. 96 (2013) 280-288.
https://doi.org/10.1002/hlca.201200386

[6] R. del Campo, J.J. Criado, E. García, M.R. Hermosa, A. Jiménez-Sánchez, J.L. Manzano, E. Monte, E. Rodríguez-Fernández, F. Sanz, J. Inorg. Biochem. 89 (2002) 74–82.
http://doi.org/10.1016/S0162-0134(01)00408-1

[7] R. Richter, J. Sieler, R. Köhler, E. Hoyer, L. Beyer, L.K. Hansen, Z. Anorg. Allg. Chem. 578 (1989) 191-197.
https://doi.org/10.1002/zaac.19895780122

[8] R. Richter, J. Sieler, R. Köhler, E. Hoyer, L. Beyer, I. Leban, L. Golič, Z. Anorg. Allg. Chem. 578 (1989) 198-204.
https://doi.org/10.1002/zaac.19895780123

[9] K.R. Koch, S.A. Bourne, A. Coetzee C, J. Miller, J. Chem. Soc. Dalton Trans., (1999) 3157–3161.
https://doi.org/10.1039/a904181h

[10] A.N. Westra, S.A. Bourne, K.R. Koch, Dalton Trans. (2005) 2916-2924.
https://10.1039/b507188g

[11] H.H Nguyen, J.J. Jegathesh, A. Takiden, D. Hauenstein, C.T. Pham, C.D. Le, U. Abram, Dalton Trans. 45 (2016) 10771-10779.
https://doi.org/10.1039/C6DT01389A

[12] C.T. Pham, H.H. Nguyen, A. Hagenbach, U. Abram, Inorg. Chem. 56 (2017) 11406-11416.
https://doi.org/10.1021/acs.inorgchem.7b01909

[13] J.J. Jesudas, C.T. Pham, A. Hagenbach, U. Abram, H.H. Nguyen, Inorg. Chem. 59 (2020) 386-395.
https://doi.org/10.1021/acs.inorgchem.9b02648

[14] N. Yang, H. Sun, Coord. Chem. Rev. 251 (2007) 2354-2366.
https://doi.org/10.1016/j.ccr.2007.03.003

[15] G.G. Briand, N. Burford, Chem. Rev. 99 (1999) 2601-2657.
https://doi.org/10.1021/cr980425s

[16] S. Wen, S.F. Moss. Cancer Lett. 282 (2009) 1-8.
https://doi.org/10.1016/j.canlet.2008.11.016

[17] S. Ahmad, A.A. Isab, S. Ali, A.R. Al-Arfaj. Polyhedron 25 (2006) 1633–1645.
http://doi.org/10.1016/j.poly.2005.11.004

[18] Y. Yang, R. Ouyang, L. Xu, N. Guo, W. Li, K. Feng, L. Ouyang, Z. Yang, S. Zhou, Y. Miao, J. Coord. Chem. 68 (2015) 379-397.
https://doi.org/ 10.1080/00958972.2014.999672

[19] R. Wang, T.-P. Lai, P. Gao, H. Zhang, P.-L. Ho, P.C.-Y. Woo, G. Ma, R.Y.-T. Kao, H. Li, H. Sun, Nat. Commun. 9 (2018) 439.
https://doi.org/10.1038/s41467-018-02828-6

[20] H. Li, R. Wang, H. Sun, Acc. Chem. Res. 52 (2019) 216−227.
https://doi.org/10.1021/acs.accounts.8b00439

[21] R. Wang, H. Li, T.K.-Y. Ip, H. Sun, Adv. Inorg. Chem. 75 (2020) 183-205.
https://doi.org/10.1016/bs.adioch.2019.10.011

[22] R.N. Duffin, M.V. Werrett, P.C. Andrews, Adv. Inorg. Chem. 75 (2020) 207-255.
https://doi.org/10.1016/bs.adioch.2019.10.001

[23] J.O. Adeyemi, D.C. Onwudiwe, Molecules 25 (2020) 305.
https://doi.org/10.3390/molecules25020305

[24] D.D. Perrin, W.L.F. Armarego, Purification of Laboratory Chemicals, fourth ed.; Butterworth-Heinemann, Oxford, 1996.

[25] M. Yokoyama, T. Ikuma, N. Obara, H. Togo, J. Chem. Soc., Perkin Trans. 1. (1990) 3243-3247.
https://doi.org/10.1039/p19900003243

[26] Bruker AXS Inc., SHELXTL XT, Version 2014/5 - Crystal Structure Solution, Madison, Wisconsin, USA, 2014.

[27] Bruker AXS Inc., SHELXTL XT, Version 2017/1 - Crystal Structure Solution, Madison, Wisconsin, USA, 2017.

[28] H. Putz, K. Brandenburg, Diamond - Crystal and Molecular Structure Visualization Bonn, Germany
http://www.crystalimpact.com/diamond

[29] CLSI. Methods for Dilution Antimicrobial Susceptibility Tests for Bacteria that Grow Aerobically (M07-A11), Clinical and Laboratory Standards Institute, Wayne P.A., 2018.

[30] I.B. Douglass, F.B. Dains, J. Am. Chem. Soc. 56 (1934) 719-721.

https://doi.org/10.1021/ja01318a057

[31] A. Rodenstein, R. Richter, R. Kirmse, Z. Anorg. Allg. Chem. 633 (2007) 1713–1717. https://doi.org/10.1002/zaac.200700181

[32] M.A.V.R. da Silva, L.M.N.B.F. Santos, B. Schröder, L. Beyer, F. Dietze, J. Chem. Thermodyn. 39 (2007) 279–283
https://doi.org/10.1016/j.jct.2006.07.007

[33] S.S. dos Santos, PhD Thesis, Universidade Federal de Santa Maria, 2011.
http://repositorio.ufsm.br/handle/1/4208

[34] Y. Li, M. Yang, M. Li, H. Yu, H. Wu, S. Xie, Bioorg. Med. Chem. Lett. 23 (2013) 2228-2292.
https://doi.org/10.1016/j.bmcl.2013.02.097

[35] K. Nomiya, K. Sekino, M. Ishikawa, A. Honda, M. Yokoyama, N.C. Kasuga, H. Yokoyama, S. Nakano, K. Onodera, J. Inorg. Biochem. 98 (2004) 601-615.
https://doi.org/10.1016/j.jinorgbio.2004.01.011

[36] M. Li, M. Yang, J. Niu, L. Zhang, S. Xie, Inorg. Chem. 51 (2012) 12521-12526.
https://doi.org/10.1021/ic301959z

[37] R. P.-Paradela, A. R.-Rodríguez, A. G.-Padula, I. Brandariz, L. Valencia, D. E.-Gómez, C. P.-Iglesias, Dalton Trans. 47 (2018) 13830-13842.
https://doi.org/10.1039/c8dt02602e

[38] L.S.-Livny, J.P. Glusker, C.W. Bock, Inorg. Chem. 37 (1998) 1853-1867
https://doi.org/10.1021/ic970909r

[39] V.G.-Montalvo, R.C.-Olivares, D.J. Williams, G.E.-Pérez, Inorg. Chem. 35 (1996) 3948-3953
https://doi.org/10.1021/ic9512082

[40] R. Luckay, I. Cukrowski, J. Mashishi, J.H. Reibenspies, A.H. Bond, R.D. Rogersand. R.D. Hancock, J. Chem. Soc., Dalton Trans. (1997) 901-908
https://doi.org/10.1039/A605068I

[41] V.D. Schwade, L. Kirsten, A. Hagenbach, E.S. Lang, U. Abram, Polyhedron 55 (2013) 155–161.
https://doi.org/10.1016/j.poly.2013.03.008

[42] C. T. Pham, M. R. Jungfer, U. Abram, New J. Chem. 44 (2020) 3672-3680.
https://doi.org/110.1039/c9nj06420f

[43] R. del Campo, J.J. Criado, R. Gheorghe, F.J. González, M.R. Hermosa, F. Sanz, J. L. Manzano, E. Monte, E. R.-Fernández, J. Inorg. Biochem. 98 (2004) 1307–1314.
http://doi.org/10.1016/j.jinorgbio.2004.03.019

[44] Z. Weiqun, Y. Wen, X. Liqun, C. Xianche, J. Inorg. Biochem. 99 (2005) 1314–1319

https://doi.org/10.1016/j.jinorgbio.2005.03.004

[45] M.T. Weller, N.A. Young, Characterisation Methods in Inorganic Chemistry, Oxford University Press, Oxford, 2017.

[46] H. Liu, W. Yang, W. Zhou, Y. Xu, J. Xie, M. Li, Inorg. Chim. Acta 405 (2013) 387-394. https://doi.org/10.1016/j.ica.2013.06.029

Tables

Table 1. Selected bond lengths (Å) and angles (º) for compound **1**.

Bond lengths (Å)		**Bond angles (º)**	
Bi1-O1	2.3704(03)	**O1-Bi1-O2**	138.350(11)
Bi1-O2	2.4072(03)	**O1-Bi1-S1**	75.215(08)
Bi1-O3	2.4070(03)	**O1-Bi1-S2**	80.803(9)
Bi1-S1	2.8287(12)	**O1-Bi1-S3**	146.572(8)
Bi1-S2	2.6192(11)	**O2-Bi1-S2**	79.018(7)
Bi1-S3	2.8462(11)	**O2-Bi1-S3**	71.923(07)
Bi1-S4	3.2147(11)	**O2-Bi1-S4**	118.792(2)
		O3-Bi1-O1	70.255(10)
		O3-Bi1-O2	143.053(10)
		O3-Bi1-S1	143.776(7)
		O3-Bi1-S2	86.097(7)
		S1-Bi1-O2	75.532(08)
		S1-Bi1-S3	137.643(4)
		S2-Bi1-S1	99.070(4)
		S2-Bi1-S3	96.052(3)
		S2-Bi1-S4	162.176(10)
		S3-Bi1-O3	76.339(07)

Table 2. Selected bond lengths (Å) and angles (º) for compound **2**.

Bond lengths (Å)		**Bond angles (º)**	
Bi1-O11	2.3140(14)	**O11-Bi1-O21**	140.150(7)
Bi1-O21	2.4245(15)	**O11-Bi1-O31**	71.670(6)
Bi1-O31	2.4998(17)	**O11-Bi1-S11**	79.200(4)
Bi1-S11	2.6955 (07)	**O11-Bi1-S33'**	70.346(04)
Bi1-S22	2.6616(08)	**O11-Bi1-S22**	79.632(5)
Bi1-S33	3.0946(07)	**O21-Bi-O31**	137.190(6)
Bi1-S33'	3.1542(07)	**O21-Bi-S22**	78.310 (4)
		O21-Bi1-S11	72.300(5)
		O21-Bi1-S33'	137.054(5)
		O31-Bi-S22	83.710 (5)
		O31-Bi1-S11	149.640(4)
		O31-Bi1-S33'	70.050(05)
		S11-Bi1-S33	146.157(3)
		S11-Bi1-S33'	92.443(18)
		S22-Bi1-S11	99.540(3)
		S22-Bi1-S33'	144.894(02)

Table 3. Selected bond lengths (Å) and angles (º) for compound **3**.

Bond lengths (Å)		**Bond angles (º)**	
Bi1-N11	2.5403(4)	**N11-Bi1-N14**	66.238(6)
Bi1-N14	2.3133(4)	**N11-Bi1-O11**	60.989(5)
Bi1-O32	2.6162(3)	**N11-Bi1-S32**	69.752(5)
Bi1···O11	2.7779(3)	**N14-Bi1-S12**	60.616(5)
Bi1-S12	2.7635(15)	**N14-Bi1-S32**	91.616(5)
Bi1-S32	2.6296(16)	**O11-Bi1-O32**	96.357(6)
Bi1···O21N'	3.1029(4)	**O11-Bi1-S32**	82.266(5)
Bi1···O22N'	2.9218(3)	**O32-Bi1-S32**	78.406(5)
Bi1···O31N	2.8025(3)	**S12-Bi1-S32**	91.709(5)
Bi2-N21	2.5300(4)	**N21-Bi2-N22**	66.794(5)
Bi2-N22	2.3100(4)	**N21-Bi2-O23**	60.780(5)
Bi2-O11	2.6761(3)	**N21-Bi2-S11**	69.432(5)
Bi2-O23	2.8016(3)	**N22-Bi2-S11**	92.431(5)
Bi2-S11	2.6150(16)	**N22-Bi2-S21**	61.119(5)
Bi2-S21	2.7420(16)	**O11-Bi2-O23**	95.380(5)
Bi2···O21N	2.9020(2)	**O11-Bi2-S11**	76.182(5)
Bi2···O23N	3.1825(2)	**O23-Bi2-S11**	79.707(5)
Bi2···O31N	3.0050(3)	**S11-Bi2-S21**	92.007(5)
Bi2···O32N	3.1002(3)		
Bi3-N31	2.5316(4)	**N31-Bi3-N32**	66.828(5)
Bi3-N32	2.3267(4)	**N31-Bi3-O32**	60.874(5)
Bi3-O23'	2.6419(3)	**N31-Bi3-S22'**	70.175(5)
Bi3···O32	2.8032(2)	**N32-Bi3-S22'**	92.156(5)
Bi3-S22'	2.6302(15)	**N32-Bi3-S31**	61.049(5)
Bi3-S31	2.7320(16)	**O23'-Bi3-O32**	94.976(5)
Bi3···O33N	3.0993(3)	**O23'-Bi3-S22'**	77.563(5)
Bi3···O22N	3.0525(3)	**O32-Bi3-S22'**	80.785(5)
Bi3···O23N	2.9413(3)	**S22'-Bi3-S31**	92.278(5)
Bi3···O31N	3.1773(4)		

Table 4. FTIR spectra main bands for the synthesized ligands and complexes.

Assignment	HL[a]	HL[b]	H_2L[c]	1	2	3
ν(O-H)[i]	-	-	-	-	-	3430
ν(N-H)	3264m	3236m	3265m	3243w	-	-
ν(C=O)	1651s	1662s	1672s	1682m[ii]	1702m[iii]	1642m[ii]
				1494s	1484s	1520s
ν(C=S)	1278m	1266s	1275m	1245m	1258m	1253m
ν(N-O)[iv]	-	-	-	-	-	1331s
						1346s

[i] H_2O solvate; [ii] non-coordinated C=O; [iii] non-coordinated C=O from acetone solvate; [iv] nitrate ions.

Table 5. Inhibition of zones (mm) and MIC values (μg mL^{-1}) of compounds against tested bacteria.

	E. coli ATCC 25922		*P. aeruginosa* ATCC 27853		*S. aureus* ATCC 25923	
Compound	**IZ**	**MIC**	**IZ**	**MIC**	**IZ**	**MIC**
HL[a]	-	>10.0	-	>10.0	-	>10.0
HL[b]	-	>10.0	-	>10.0	-	>10.0
H_2L[c]	-	>10.0	-	>10.0	-	>10.0
1	-	>10.0	-	>10.0	-	>10.0
2	-	0.156	13.0	1.250	12.0	0.019
3	-	5.0	-	2.5	-	2.5
$Bi(NO_3)_3 \cdot 5H_2O$	-	>10.0	-	5.0	-	>10.0

IZ: inhibition zones; MIC: minimum inhibitory concentration. The "-" signals indicate no inhibition zone observed.

Figures

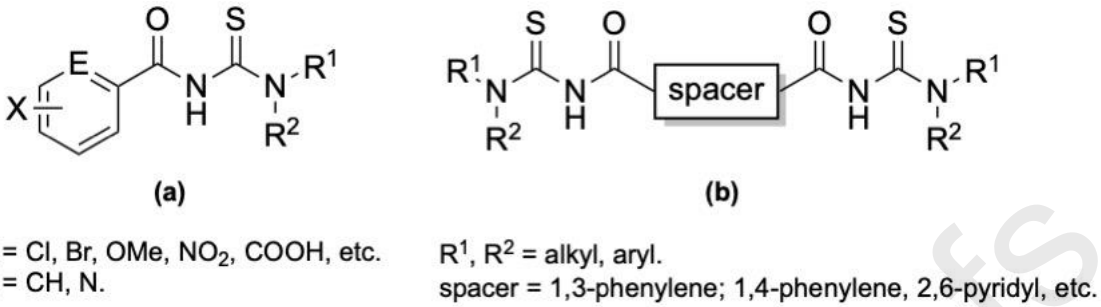

Figure 1. Molecular structures of: **(a)** monopodal aroylthioureas; **(b)** bipodal aroylthioureas.

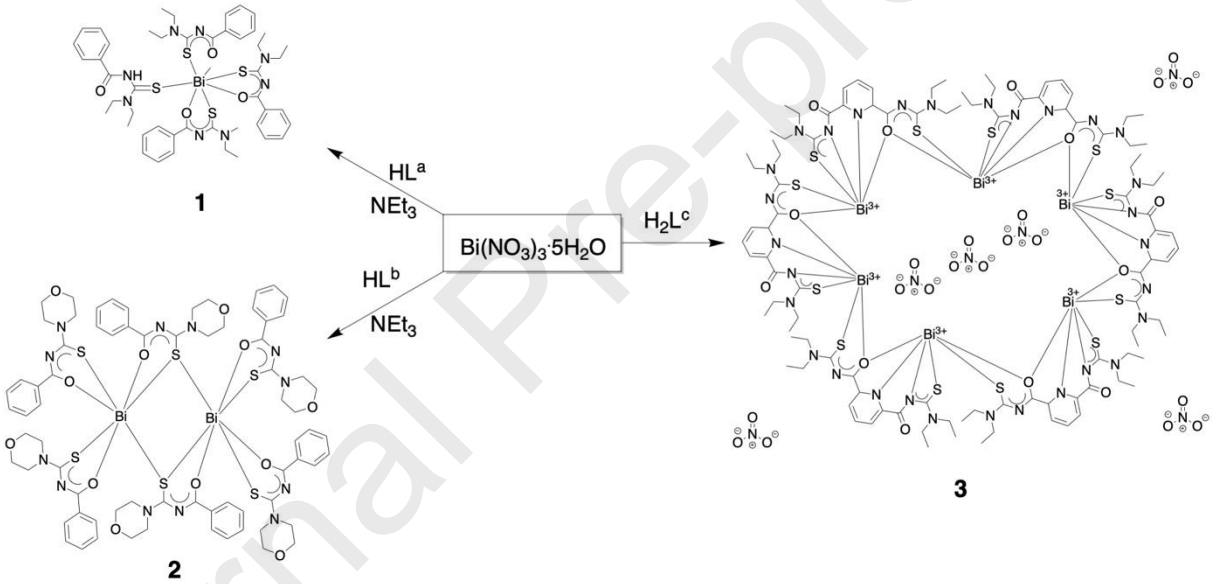

Figure 2. Schematic route to obtain complexes **1 – 3**, with HL^a = *N*-benzoyl(*N',N'*-diethylthiourea), HL^b = *N*-benzoyl(morpholinylthiourea), and H_2L^c = N^2,N^6-bis(diethylcarbamothioyl)pyridine-2,6-dicarboxamide. Solvate molecules are omitted in this representation.

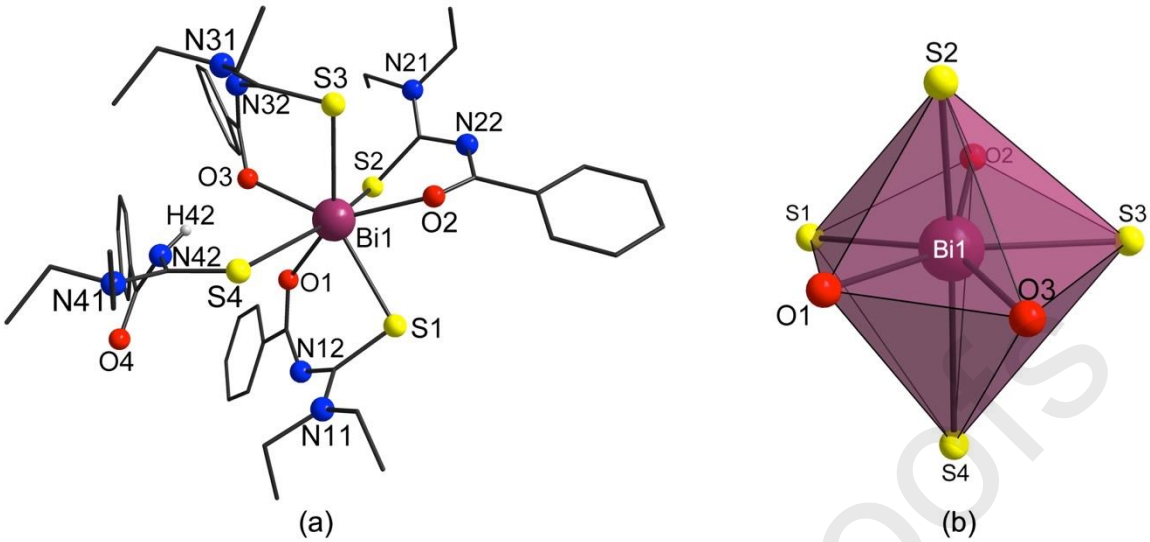

Figure 3. (a) Molecular structure of **1** (hydrogen atoms attached to carbon were omitted for clarity). (b) Coordination environment for bismuth(III) in compound **1**.

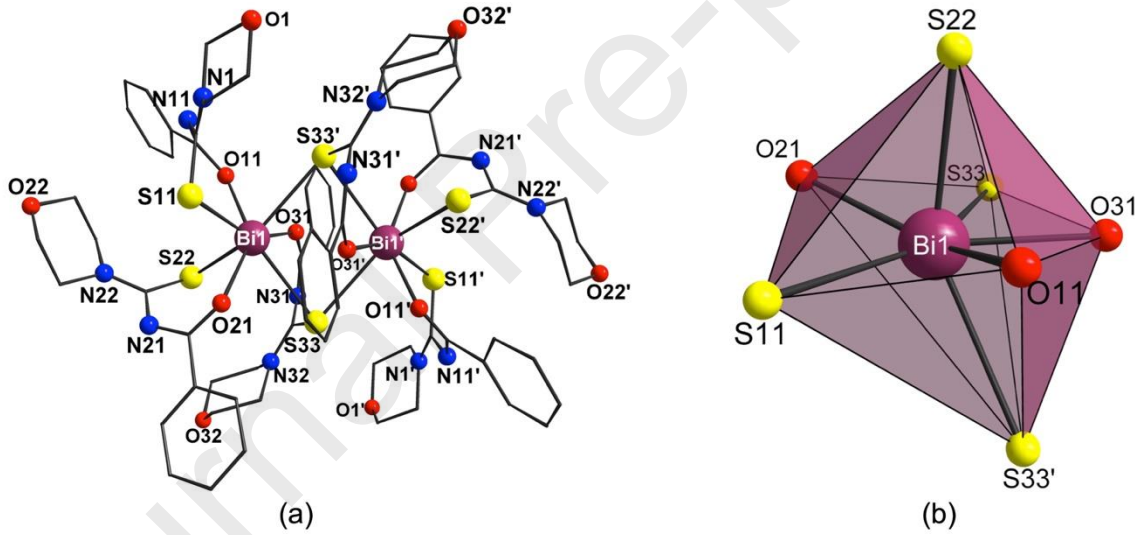

Figure 4. (a) Molecular structure of **2** (hydrogen atoms and solvate molecules were omitted for clarity). (b) Coordination geometry around bismuth in complex **2**. Symmetry operations used to generate equivalent atoms: ' = *–x*, *–y*, *–z*.

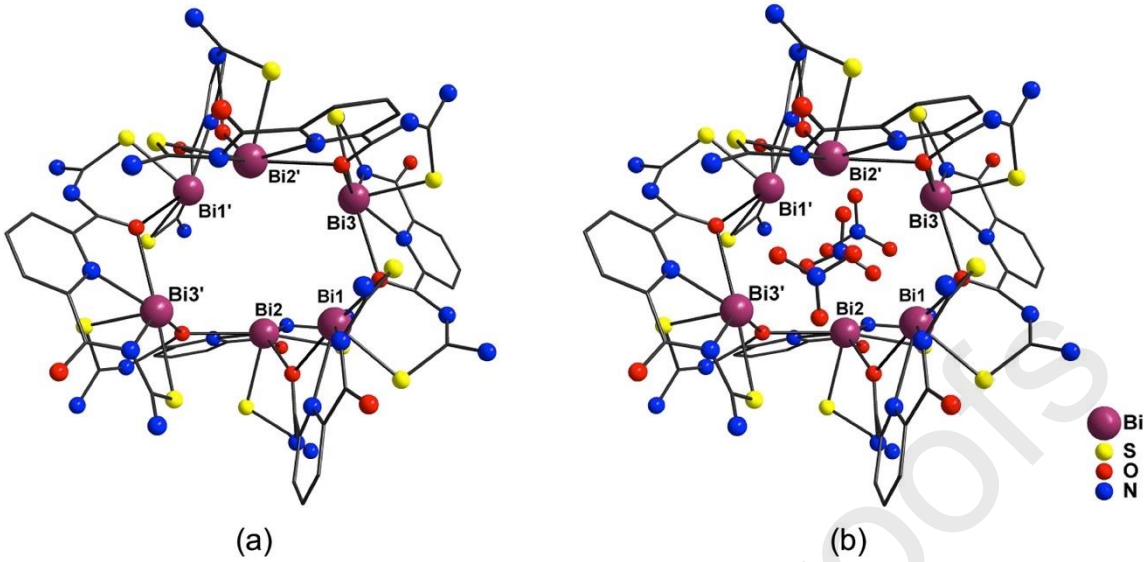

Figure 5. Two different projections of the molecular structure of **3**: (a) the cationic fragment built up by Bi^{III} and L^{c} moieties, with emphasis in the central void; (b) the cationic framework and the encapsulated nitrate ions. Hydrogen atoms, ethyl groups, solvate molecules, and peripheral nitrate counterions were omitted for clarity. Symmetry operations used to generate equivalent atoms: ' = 1–*x*, 1–*y*, 1–*z*.

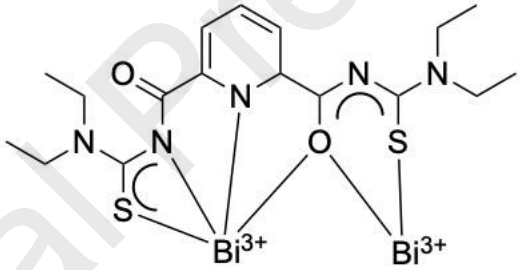

Figure 6. Representation of the coordination scheme provided by the ligands L^{c} in compound **3**, with emphasis in the distinct chelating systems to two adjacent bismuth(III) ions.

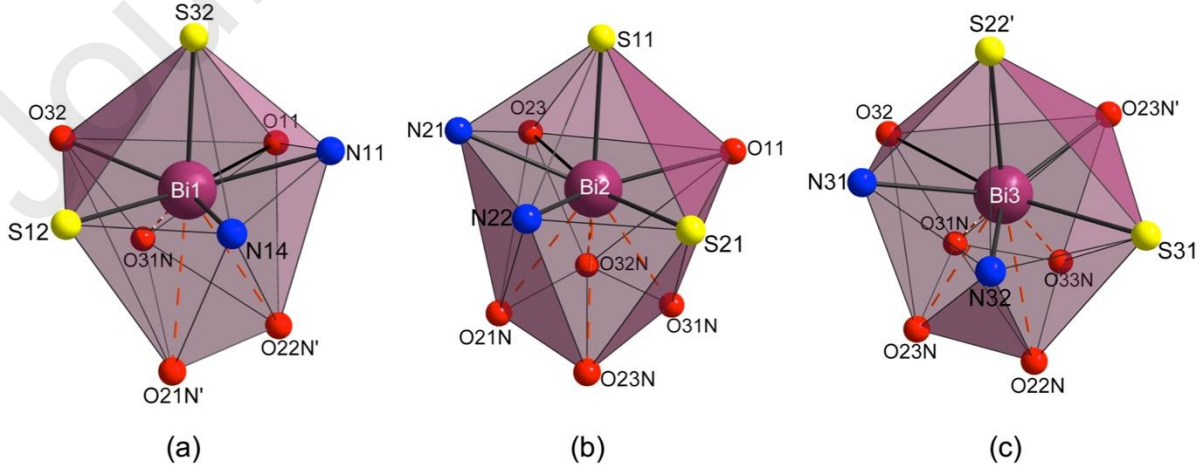

Figure 7. The coordination environments of the independent Bi^{III} species in compound **3**. Symmetry operations used to generate equivalent atoms: ' = 1–*x*, 1–*y*, 1–*z*.

Table 1. Selected bond lengths (Å) and angles (º) for compound **1**.

Bond lengths (Å)		**Bond angles (º)**	
Bi1-O1	2.3704(03)	**O1-Bi1-O2**	138.350(11)
Bi1-O2	2.4072(03)	**O1-Bi1-S1**	75.215(08)
Bi1-O3	2.4070(03)	**O1-Bi1-S2**	80.803(9)
Bi1-S1	2.8287(12)	**O1-Bi1-S3**	146.572(8)
Bi1-S2	2.6192(11)	**O2-Bi1-S2**	79.018(7)
Bi1-S3	2.8462(11)	**O2-Bi1-S3**	71.923(07)
Bi1-S4	3.2147(11)	**O2-Bi1-S4**	118.792(2)
		O3-Bi1-O1	70.255(10)
		O3-Bi1-O2	143.053(10)
		O3-Bi1-S1	143.776(7)
		O3-Bi1-S2	86.097(7)
		S1-Bi1-O2	75.532(08)
		S1-Bi1-S3	137.643(4)
		S2-Bi1-S1	99.070(4)
		S2-Bi1-S3	96.052(3)
		S2-Bi1-S4	162.176(10)
		S3-Bi1-O3	76.339(07)

Table 2. Selected bond lengths (Å) and angles (º) for compound **2**.

Bond lengths (Å)		**Bond angles (º)**	
Bi1-O11	2.3140(14)	**O11-Bi1-O21**	140.150(7)
Bi1-O21	2.4245(15)	**O11-Bi1-O31**	71.670(6)
Bi1-O31	2.4998(17)	**O11-Bi1-S11**	79.200(4)
Bi1-S11	2.6955 (07)	**O11-Bi1-S33'**	70.346(04)
Bi1-S22	2.6616(08)	**O11-Bi1-S22**	79.632(5)
Bi1-S33	3.0946(07)	**O21-Bi-O31**	137.190(6)
Bi1-S33'	3.1542(07)	**O21-Bi-S22**	78.310 (4)
		O21-Bi1-S11	72.300(5)
		O21-Bi1-S33'	137.054(5)
		O31-Bi-S22	83.710 (5)
		O31-Bi1-S11	149.640(4)
		O31-Bi1-S33'	70.050(05)
		S11-Bi1-S33	146.157(3)

		S11-Bi1-S33'	92.443(18)
		S22-Bi1-S11	99.540(3)
		S22-Bi1-S33'	144.894(02)

Table 3. Selected bond lengths (Å) and angles (º) for compound **3**.

Bond lengths (Å)		**Bond angles (º)**	
Bi1-N11	2.5403(4)	**N11-Bi1-N14**	66.238(6)
Bi1-N14	2.3133(4)	**N11-Bi1-O11**	60.989(5)
Bi1-O32	2.6162(3)	**N11-Bi1-S32**	69.752(5)
Bi1···O11	2.7779(3)	**N14-Bi1-S12**	60.616(5)
Bi1-S12	2.7635(15)	**N14-Bi1-S32**	91.616(5)
Bi1-S32	2.6296(16)	**O11-Bi1-O32**	96.357(6)
Bi1···O21N'	3.1029(4)	**O11-Bi1-S32**	82.266(5)
Bi1···O22N'	2.9218(3)	**O32-Bi1-S32**	78.406(5)
Bi1···O31N	2.8025(3)	**S12-Bi1-S32**	91.709(5)
Bi2-N21	2.5300(4)	**N21-Bi2-N22**	66.794(5)
Bi2-N22	2.3100(4)	**N21-Bi2-O23**	60.780(5)
Bi2-O11	2.6761(3)	**N21-Bi2-S11**	69.432(5)
Bi2-O23	2.8016(3)	**N22-Bi2-S11**	92.431(5)
Bi2-S11	2.6150(16)	**N22-Bi2-S21**	61.119(5)
Bi2-S21	2.7420(16)	**O11-Bi2-O23**	95.380(5)
Bi2···O21N	2.9020(2)	**O11-Bi2-S11**	76.182(5)
Bi2···O23N	3.1825(2)	**O23-Bi2-S11**	79.707(5)
Bi2···O31N	3.0050(3)	**S11-Bi2-S21**	92.007(5)
Bi2···O32N	3.1002(3)		
Bi3-N31	2.5316(4)	**N31-Bi3-N32**	66.828(5)
Bi3-N32	2.3267(4)	**N31-Bi3-O32**	60.874(5)
Bi3-O23'	2.6419(3)	**N31-Bi3-S22'**	70.175(5)
Bi3···O32	2.8032(2)	**N32-Bi3-S22'**	92.156(5)

Bi3-S22'	2.6302(15)	**N32-Bi3-S31**	61.049(5)
Bi3-S31	2.7320(16)	**O23'-Bi3-O32**	94.976(5)
Bi3···O33N	3.0993(3)	**O23'-Bi3-S22'**	77.563(5)
Bi3···O22N	3.0525(3)	**O32-Bi3-S22'**	80.785(5)
Bi3···O23N	2.9413(3)	**S22'-Bi3-S31**	92.278(5)
Bi3···O31N	3.1773(4)		

Table 4. FTIR spectra main bands for the synthesized ligands and complexes.

Assignment	HL[a]	HL[b]	H_2L[c]	1	2	3
ν(O-H)[i]	-	-	-	-	-	3430
ν(N-H)	3264m	3236m	3265m	3243w	-	-
ν(C=O)	1651s	1662s	1672s	1682m[ii]	1702m[iii]	1642m[ii]
				1494s	1484s	1520s
ν(C=S)	1278m	1266s	1275m	1245m	1258m	1253m
ν(N-O)[iv]	-	-	-	-	-	1331s
						1346s

[i] **H_2O solvate;** [ii] **non-coordinated C=O;** [iii] **non-coordinated C=O from acetone solvate;** [iv] **nitrate ions.**

Table 5. Inhibition of zones (mm) and MIC values (μg mL^{-1}) of compounds against tested bacteria.

	E. coli **ATCC 25922**		***P. aeruginosa*** **ATCC 27853**		***S. aureus*** **ATCC 25923**	
Compound	**IZ**	**MIC**	**IZ**	**MIC**	**IZ**	**MIC**
HL[a]	-	>10.0	-	>10.0	-	>10.0
HL[b]	-	>10.0	-	>10.0	-	>10.0
H_2L[c]	-	>10.0	-	>10.0	-	>10.0
1	-	>10.0	-	>10.0	-	>10.0
2	-	0.156	13.0	1.250	12.0	0.019
3	-	5.0	-	2.5	-	2.5
$Bi(NO_3)_3 \cdot 5H_2O$	-	>10.0	-	5.0	-	>10.0

IZ: inhibition zones; MIC: minimum inhibitory concentration. The "-" signals indicate no inhibition zone observed.

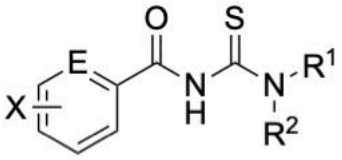

(a)

X = Cl, Br, OMe, NO_2, COOH, etc.
E = CH, N.

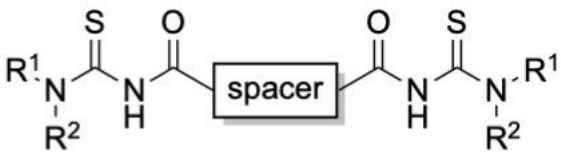

(b)

R^1, R^2 = alkyl, aryl.
spacer = 1,3-phenylene; 1,4-phenylene, 2,6-pyridyl, etc.

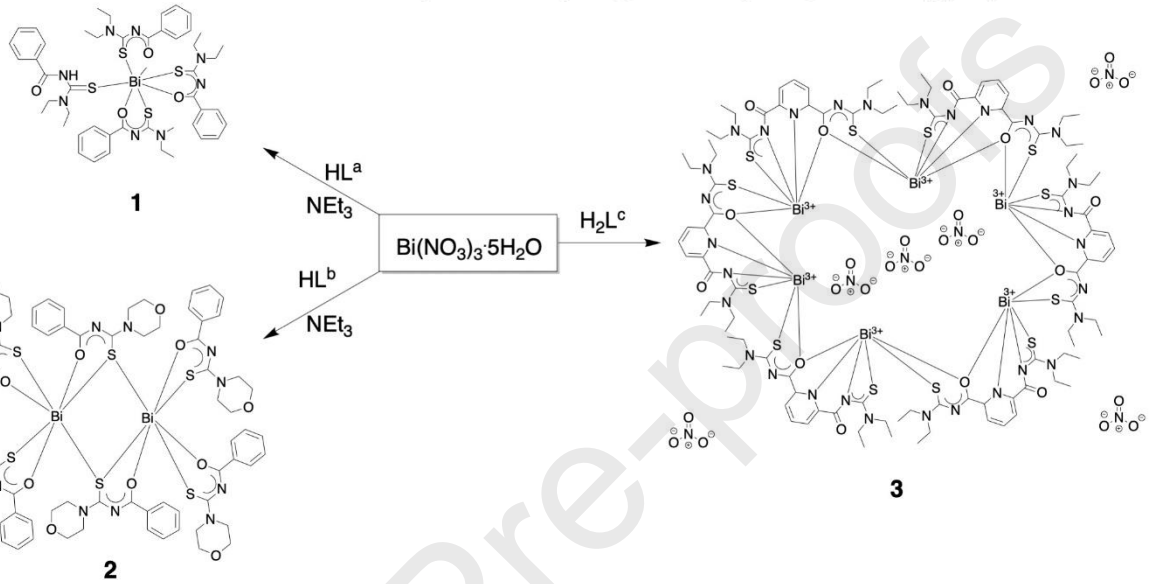

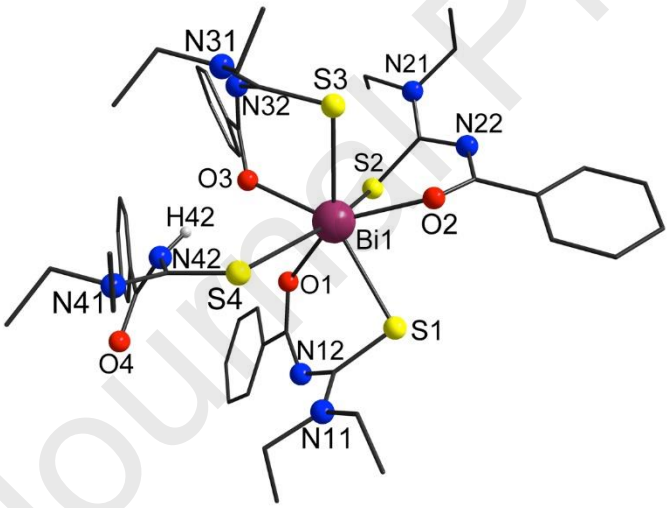

(a)

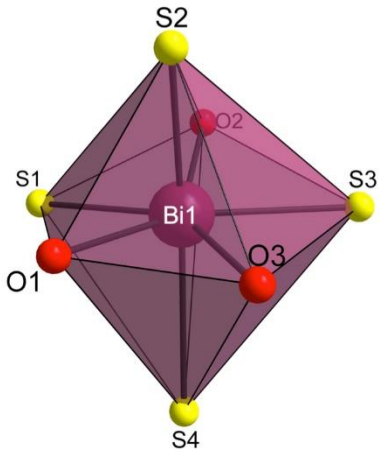

(b)

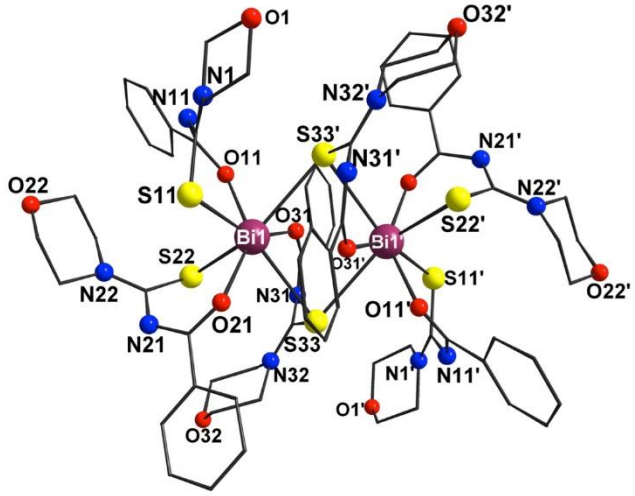

(a)

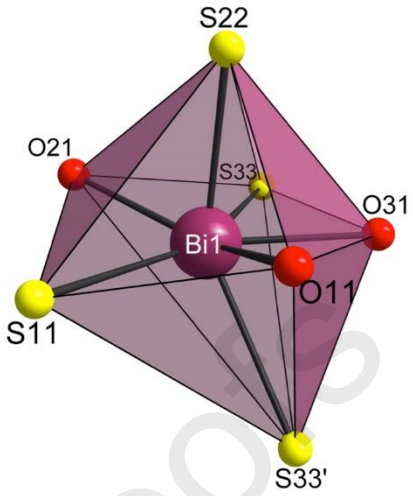

(b)

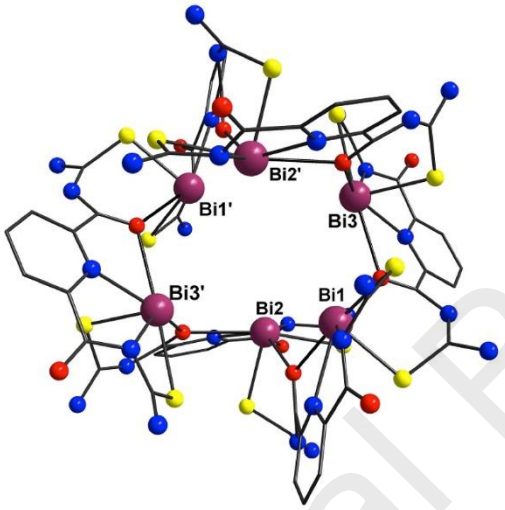

(a)

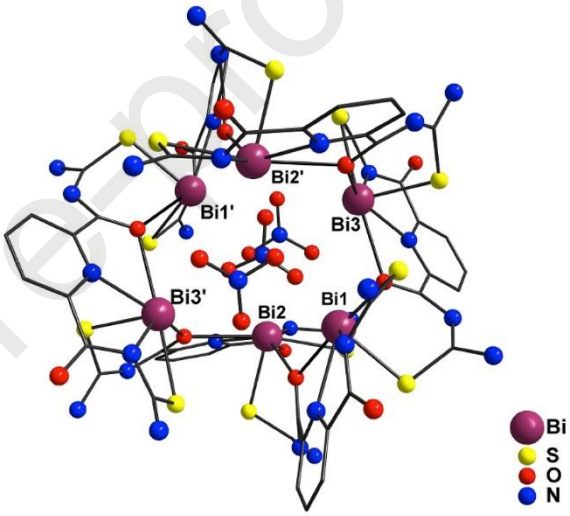

(b)

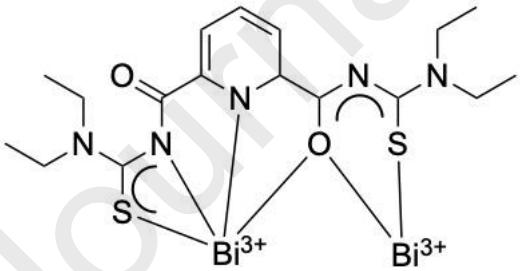

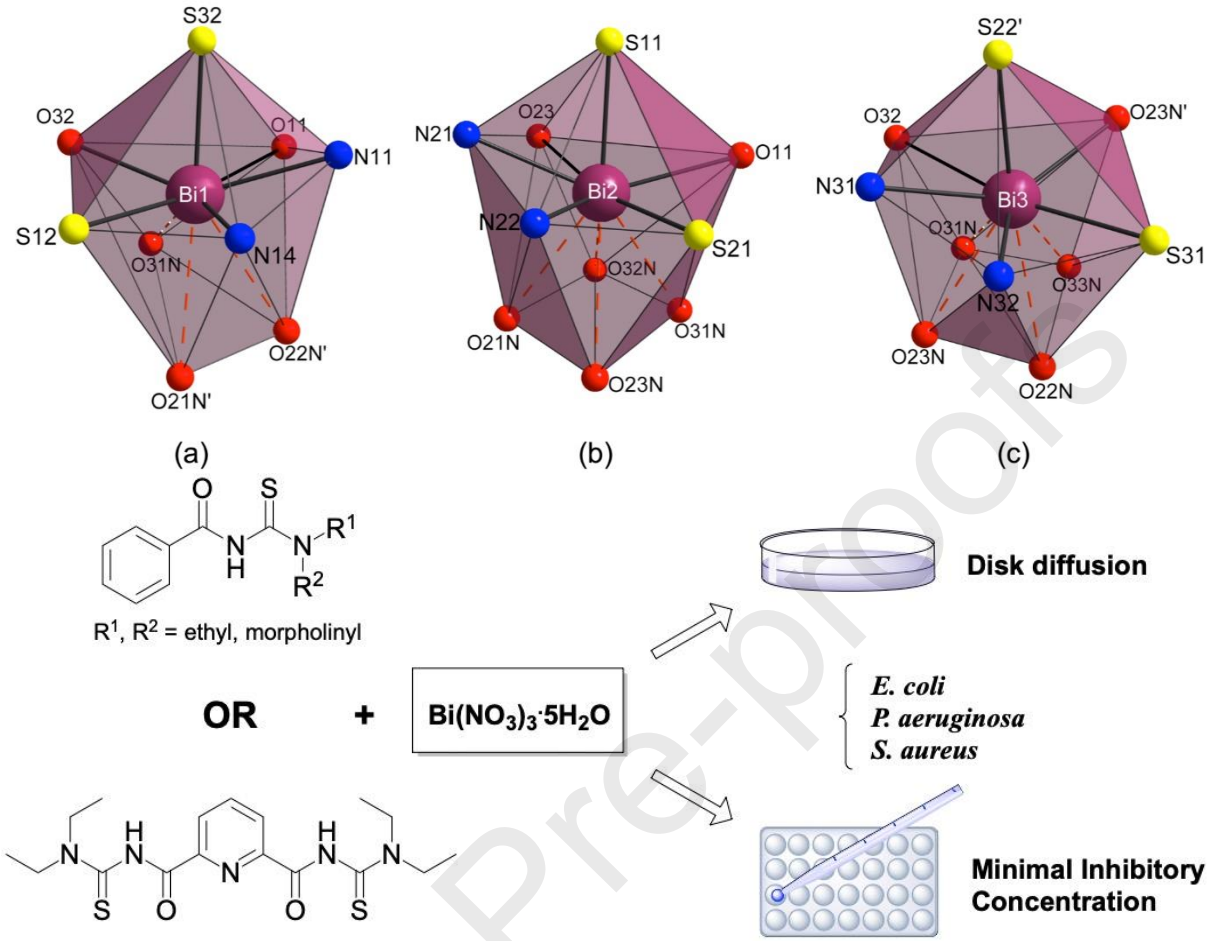

Synthesis, characterization and biological applications of bismuth(III) complexes with aroylthiourea ligands

Marcielli Indiara de Oliveira, Gabriela Pereira Chuy, Bruno Stefanello Vizzotto, Robert Alan Burrow, Ernesto Schulz Lang and Sailer Santos dos Santos*